Annals of Biomedical Engineering (© 2018)
https://doi.org/10.1007/s10439-018-1981-2

Real-Time Closed Loop Diastolic Interval Control Prevents Cardiac Alternans in Isolated Whole Rabbit Hearts

KANCHAN KULKARNI, STEVEN W. LEE, RYAN KLUCK, and ELENA G. TOLKACHEVA

Department of Biomedical Engineering, University of Minnesota, 6-128 Nils Hasselmo Hall, 312 Church St. SE, Minneapolis, MN 55455, USA

(*Received 30 July 2017; accepted 12 January 2018*)

Associate Editor Ellen Kuhl oversaw the review of this article.

Abstract—Cardiac alternans, a beat-to-beat alternation in action potential duration (*APD*), can lead to fatal arrhythmias. During periodic pacing, changes in diastolic interval (*DI*) depend on subsequent changes in *APD*, thus enhancing cardiac instabilities through a 'feedback' mechanism. Recently, an anti-arrhythmic *Constant DI* pacing protocol was proposed and shown to be effective in suppressing alternans in 0D and 1D *in silico* studies. However, previous experimental validation of *Constant DI* pacing in the heart has been unsuccessful due to the spatio-temporal complexity of 2D cardiac tissue and the technical challenges in its real-time implementation. Here, we developed a novel closed loop system to detect T-waves from real-time ECG data, enabling successful implementation of *Constant DI* pacing protocol, and performed high-resolution optical mapping experiments on isolated whole rabbit hearts to validate its anti-arrhythmic effects. The results were compared with: (1) *Periodic* pacing (feedback inherent) and (2) pacing with heart rate variability (*HRV*) (feedback modulation) introduced by using either *Gaussian* or *Physiological* patterns. We observed that *Constant DI* pacing significantly suppressed alternans in the heart, while maintaining *APD* spatial dispersion and flattening the slope of the *APD* restitution curve, compared to traditional *Periodic* pacing. In addition, introduction of *HRV* in *Periodic* pacing failed to prevent cardiac alternans, and was arrhythmogenic.

Keywords—Optical mapping, Arrhythmias, Pacing, Beat-to-beat, HRV, Periodic.

INTRODUCTION

Fatal arrhythmias and ventricular fibrillation (VF) which lead to sudden cardiac death are often preceded by alternans, a beat-to-beat alternation in the cellular action potential duration (*APD*).[6,10,15,29] *APD* alternans often manifest as T-wave alternans, an alternation in the shape or duration of the T-wave, in an electrocardiogram (ECG). When the heart is paced at progressively increasing rates, electrical restitution, which is a fundamental property of cardiac myocytes, causes the heart to transition from a constant *APD* response at lower frequencies to an alternating long-short *APD* pattern (alternans) at higher frequencies.[22,27] Although important for life at moderate heart rates, at higher rates, restitution may result in life-threatening cardiac rhythms such as alternans. Multiple mechanisms have been suggested to be responsible for the onset of cardiac alternans, from restitution dependent electrical instabilities to intracellular calcium cycling abnormalities.[26,27] It is hypothesized that alternans is a precursor of cardiac electrical instability and previous studies have established a plausible link between alternans and ventricular arrhythmias, suggesting that elimination of alternans could lead to the prevention of VF and eventual arrhythmias in the heart.[10,15,21,25]

Over the past two decades, several groups have attempted the control of alternans through *in silico*, *in vitro* and *ex vivo* experiments.[2–5,7–9,11–14,18–20,31] Although early studies reported positive results in single cell models and *in vitro* preparations,[11,12] control of alternans in more spatiotemporally complex two-dimensional (2D) settings has proved unsuccessful.[5,30] Many groups since have highlighted the significant challenges in the spatiotemporal control of cardiac alternans, revealing that control failed above a critical cable length[5,9] and became attenuated spatially as alternans amplitude increased.[4,13,30] However, a major flaw in the control algorithms was the use of periodic stimulation, wherein the duration between consecutive

Address correspondence to Elena G. Tolkacheva, Department of Biomedical Engineering, University of Minnesota, 6-128 Nils Hasselmo Hall, 312 Church St. SE, Minneapolis, MN 55455, USA. Electronic mail: talkacal@umn.edu

Published online: 22 January 2018

stimuli (basic cycle length (*BCL*)) is constant from beat-to-beat, i.e.,

$$APD_n + DI_n = BCL_n = BCL = \text{constant} \quad (1)$$

where n is the stimulus number and DI_n denotes the nth diastolic interval (the cardiac relaxation phase). During periodic pacing (Eq. (1)), there is a partial dependence of the *DI* on the preceding *APD* ($DI_n = BCL - APD_n$), i.e., *feedback*, that can lead to subsequent destabilization of normal cardiac rhythms.[18,31] We recently reported the drawbacks of periodic pacing using single cell and 1D cable numerical simulations,[18,31] in comparison to the beneficial anti-arrhythmic effects of feedback elimination by keeping the *DI* constant, i.e.,

$$DI_n = DI = \text{constant} \quad (2)$$

Indeed, by controlling and maintaining a *Constant DI* on a beat-by-beat basis, we eliminated feedback and the inherent dependence of the *DI* on the preceding *APD*, which was successful in suppressing alternans.[18,31] More recently though, contradictory findings demonstrating the presence of alternans *in silico* during *Constant DI* pacing was reported by some groups,[2,19] particularly under abnormal calcium cycling conditions. In addition, closed loop experimental validation of beat-to-beat control of alternans has exhibited limited success, especially in 2D cardiac tissue preparations.[14,30] Experimental implementation of *Constant DI* pacing is challenging and previous attempts involving the control of *DI* were limited to point sensing using microelectrodes which failed to address the prevention of alternans in the heart.[30] In order to precisely control the *DI* in the whole heart, on a beat-to-beat basis, there is a need to develop a sophisticated control algorithm that can sense an action potential in real-time based on comprehensive cardiac electrical information, and apply a stimulus after a predefined time interval at the end of the *APD*.

The main goal of the current study was to develop a real-time beat-to-beat control system to successfully implement *Constant DI* pacing and demonstrate its efficacy in suppressing alternans in the whole heart. We successfully addressed the technical limitations mentioned previously and implemented a novel method to validate the anti-arrhythmic benefits of feedback elimination using *Constant DI*, in *ex vivo* isolated whole rabbit hearts. Specifically, we implemented a closed loop algorithm to detect T-waves from real-time ECG data on a beat-by-beat basis, measure real-time *APD* and apply stimuli after a predefined *Constant DI*. To our knowledge, this is the first study to use whole heart 2D optical mapping for high resolution spatio-temporal assessment of feedback between *DI* and *APD*. In addition, we compared the electrophysiological and anti-arrhythmic effects of *Constant DI* pacing with different pacing protocols. Namely, the following protocols were used: (1) *Periodic* pacing (feedback inherent), (2) *HRV* pacing (feedback modulation), introduced by using both (2.1) *Gaussian* and (2.2) *Physiological* variability patterns, and (3) *Constant DI* pacing (feedback eliminated).

METHODS

Optical Mapping

All experiments were performed in accordance with the guidelines of the Institutional Animal Care and Use Committee at the University of Minnesota. Optical mapping procedures were performed as previously described.[16,28] Briefly, New Zealand White rabbits (Bakkom Rabbitry, 1.3–2.0 kg, $n = 8$) were injected with heparin sulfate (550 U/100 g) and anesthetized with ketamine and xylazine (35 and 5 mg/kg, resp.). The heart was quickly excised after a thoracotomy and immersed in cold cardioplegic solution (in mM: glucose 280, KCl 13.44, $NaHCO_3$ 12.6, and mannitol 34). The aorta was quickly cannulated and retrogradely perfused with warm (37 ± 1 °C) oxygenated Tyrode's solution (in mM: NaCl 130, $CaCl_2$ 1.8, KCl 4, $MgCl_2$ 1.0, NaH_2PO_4 1.2, $NaHCO_3$ 24, glucose 5.5, and pH 7.4) under constant pressure. The heart was immersed in a chamber and superfused with the same Tyrode's solution. Motion uncoupler Blebbistatin (10 μM) was added to Tyrode's solution when needed to reduce motion artifacts.

A bolus of 4 mL of the voltage-sensitive dye di-4-ANEPPS (10 μM) was injected and the heart was excited with a diode pumped, continuous-excitation green laser (532 nm, 1 W; Shanghai Dream Lasers Technology, Shanghai, China). Optical movies corresponding to the fluorescence signal were recorded from the epicardial surfaces of the left or right ventricle (LV and RV) at 1000 frames per second, with 14-bit, 80 × 80-pixel resolution cameras (Little Joe, RedShirt Imaging, SciMeasure) after a period of stabilization of approximately 30 min. Simultaneously, continuous 3-electrode volume conducted ECG was recorded throughout the experiments.

Real-Time Closed Loop Control Algorithm

Figure 1a shows a schematic of the setup interfacing the real-time ECG-based *Constant DI* control algorithm with high-resolution optical mapping system. We utilized RT intervals on the ECG to approximate an *APD*, while the TR interval was maintained con-

stant to implement *Constant DI*. However, as the correspondence between RT, TR intervals and *APD*, *DI*s respectively has been well established,[18] fundamentally our method implements feedback elimination by controlling the repolarization interval (for details, see Supplementary materials). Arrows in black indicate the original optical mapping set up that was used for the *Periodic* and *HRV* pacing implementation. Arrows in red indicate the closed loop system that enables real-time T-wave detection from ECG and implementation of *Constant DI* pacing. *Constant DI* pacing was implemented using a proprietary algorithm developed in LabVIEW that detected the ECG T-wave peak and applied a pacing stimulus after a predefined fixed duration equivalent to the required *DI*.

Pacing Protocols

The following pacing protocols were implemented.

Periodic Pacing Protocol

Since *Periodic* pacing (Eq. (1)) forces the *BCL* to be constant during each beat, it creates an inherent dependency of the *DI* on the preceding *APD*, i.e., feedback. Hence, in this study, we refer to *Periodic* pacing protocol as the *'feedback inherent'* protocol.

HRV Pacing Protocol

Under normal physiological conditions, there exists intrinsic *HRV*, which ensures deviation of the heart from periodic pacing.[17,24] To simulate known healthy

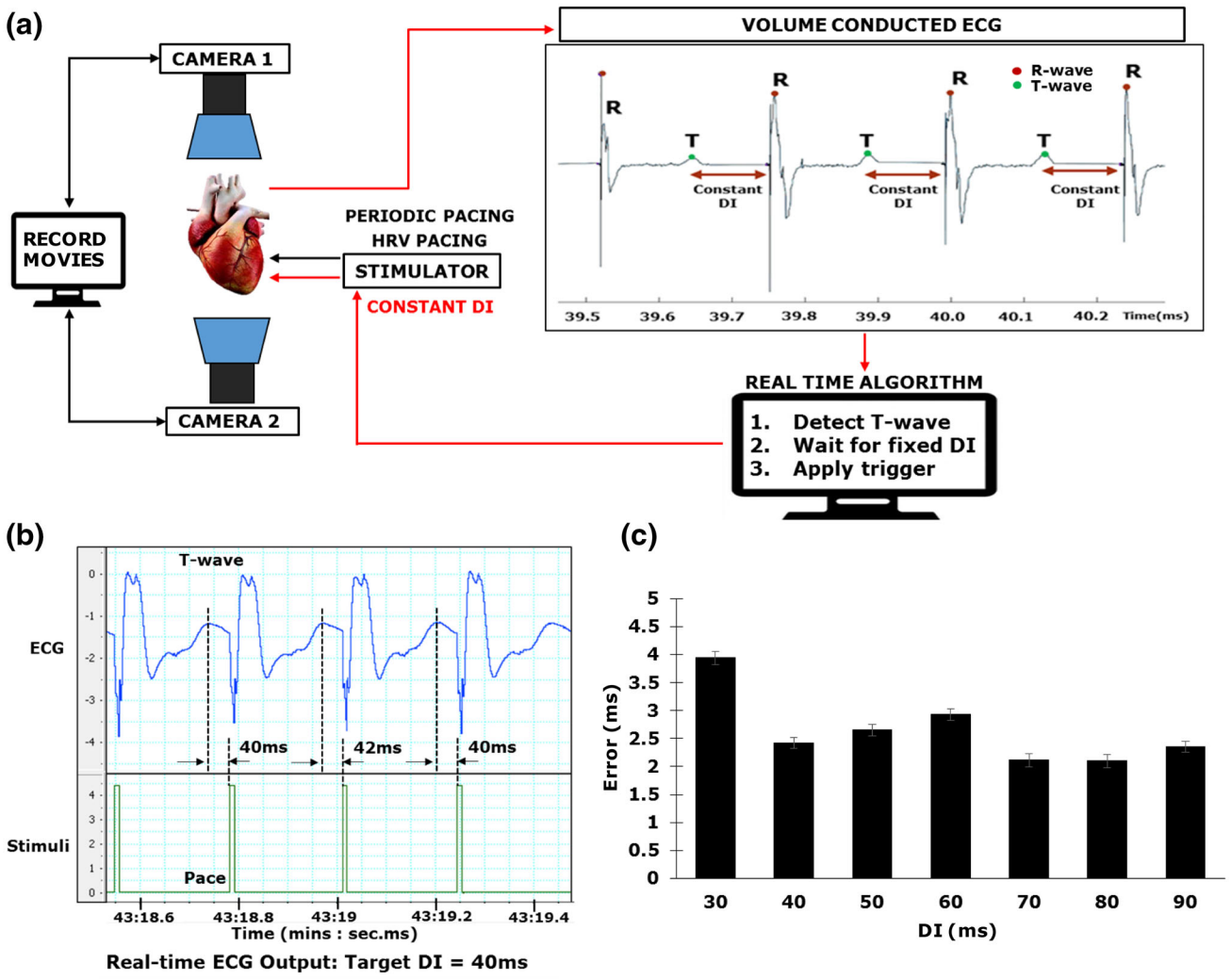

FIGURE 1. (a) Schematic of our optical mapping system for real-time closed loop control of alternans. Red arrows highlight the real-time ECG T-wave detection and *Constant DI* algorithm implementation. Black arrows indicate 2D optical imaging and implementation of *Periodic* and *HRV* pacing. (b) Validation of *Constant DI* pacing using real-time ECG recording for representative target *DI* = 40 ms. The interval between dashed vertical lines represent achieved *DI* values. Green marks represent implemented *Constant DI* pacing. (c) Error, calculated as difference between achieved and target *DI*, is shown for the entire *DI* range, for one representative pacing run.

human *HRV* and to in turn modulate the feedback between *DI* and *APD*, we incorporated stochasticity in pacing by varying the *BCL*s. Two different *HRV* pacing protocols were used to generate *'feedback modulation'*.

Gaussian Pacing Here, we incorporated *HRV* in pacing by using a strictly Gaussian distribution of beat-to-beat intervals. *Gaussian* pacing was implemented as follows:

$$BCL_n = BCL_0 \pm \delta(HRV) \tag{3}$$

where $\delta(HRV)$ is a random number with a mean of zero and standard deviation of $BCL_0{*}HRV$, and,

$$HRV = \frac{STD_{\mathrm{RR}}}{AVG_{\mathrm{RR}}} \times 100\% \tag{4}$$

where STD_{RR} and AVG_{RR} denote the standard deviation and average of the RR intervals, i.e., the distance between the RR peaks in the ECG. To mimic known human *HRV* values[18,23] we used a Gaussian distribution with *HRV* set at 5%.

Physiological Pacing Here, to mimic a physiological HRV pattern, we utilized the variation in RR intervals from a previously acquired anesthetized *in vivo* rat ECG recording. The original HRV of 1.12% was scaled up to 5% to simulate a quasi-physiologically relevant human HRV value, and the scaled RR 'pattern' was superimposed onto BCL values to implement *Physiological* pacing for each BCL from 200 ms down to 120 ms in steps of 10 ms.

Constant DI Pacing Protocol

To evaluate the proposed anti-arrhythmic effects of '*feedback elimination*', we implemented *Constant DI* pacing as shown in Eq. (2). The details of the algorithm implementation are presented in Supplementary Materials.

External stimuli at twice the activation threshold were applied at the base of the LV for each rabbit during each pacing protocol. One hundred stimuli were applied at each *BCL* for *Periodic* and *HRV* pacing, and the *BCL* was progressively decreased from 200 ms down to 120 ms in steps of 10 ms. Similarly, during *Constant DI*, 100 stimuli were applied at each *DI* and the *DI* was progressively decreased from 100 ms down to 30 ms in steps of 10 ms. It should be noted that since we aimed to investigate the propensity of the pacing techniques to the onset of alternans rather than VF, we did not perform pacing below $BCL = 120$ ms to preclude the heart to go to VF.

A total of $n = 40$ pacing runs were analyzed for both LV and RV for the *Periodic, Gaussian, Physiological* and *Constant DI* pacing protocols (10 runs of each protocol). Runs of each pacing protocol were acquired in each rabbit in a random manner, to eliminate any effect of pacing order on the results. Optical movies corresponding to the last ten stimuli were recorded for each *BCL*/ *DI* for all pacing protocols.

Data Analysis

APD Alternans

Optical movies were recorded from the epicardial surfaces of both the LV and RV. Mean *APD* at 80% repolarization ($\langle APD_{80}\rangle$) was calculated for RV and LV for the even (APD_{EVEN}) and odd (APD_{ODD}) beats separately. 2D mean APD_{EVEN} and APD_{ODD} maps were generated for each *BCL* and *DI*. Temporal threshold for alternans was set at $|APD_{\mathrm{EVEN}} - APD_{\mathrm{ODD}}| = 4$ ms and 2D alternans maps were generated as a difference of mean APD_{EVEN} and APD_{ODD} maps. For spatial onset of alternans, the *BCL* (or *DI*) at which at least 20% of the area of the RV or LV was occupied by alternans was defined as the BCL_{onset} (or DI_{onset}). The presence of spatial alternans was then quantified for all the pacing runs.

APD Heterogeneity

To assess the dispersion of APD_{80} repolarization across the LV and RV surfaces, we calculated APD_{80} heterogeneity index μ as follows:

$$\mu = \left(APD^{95} - APD^{5}\right)/APD^{50} \tag{5}$$

wherein, APD^{95} and APD^{5} represent the 95th and 5th percentiles of the APD_{80} distribution, respectively, and APD^{50} is the median of the distribution. For each *BCL* and *DI*, heterogeneity μ was calculated based on 2D *APD* maps generated for an average APD_{80} of 3–5 beats.

Comparison Between BCL and DI

In order to compare data between the different pacing protocols, the corresponding *DI* for each *BCL* was calculated for each *Periodic* and *HRV* pacing run as follows:

$$DI = BCL - \langle APD_{80}\rangle \tag{6}$$

wherein, $\langle APD_{80}\rangle = \langle (APD_{\mathrm{EVEN}},\ APD_{\mathrm{ODD}})\rangle$. Finally, mean *DI* values corresponding to each *BCL* were calculated for the *Periodic* and *HRV* pacing protocols by combining *DI* values for individual runs.

Slopes of APD Restitution Curve (S_{max})

To evaluate the effect of the different pacing protocols on the slope of the *APD* restitution curve, and in turn the propensity to arrhythmias, we calculated the minimum *DI* ($DI_{\min}$) for every pacing run (*DI* corresponding to the last *BCL* for each run). *APD* restitution curves were generated as a function of change in $\langle APD_{80} \rangle$ with *DI* and fit with a 2nd degree polynomial function. The maximum slope of restitution, $S_{\max}$, was calculated for each run by evaluating the derivative of the polynomial fit at $DI_{\min}$. Finally, the individual mean $S_{\max}$ values, corresponding to change in 2D $\langle APD_{80} \rangle$ with *DI*, for each pacing run were combined to generate average $S_{\max}$ values for each pacing protocol.

Statistics

All data are presented as mean ± standard error. Statistical comparisons between the pacing protocols were performed using 1-way ANOVA (Origin Software, Northampton, MA, USA). Fisher's exact test was used to perform statistical comparison of the number of runs that exhibited arrhythmias across the different pacing protocols. Values of $p < 0.05$ were considered statistically significant.

RESULTS

Real-Time T-Wave Measurements

We first validated accurate T-wave detection by the real-time algorithm and execution of *Constant DI* pacing. The time instances of each T-wave peak detected and pacing stimulus applied was generated by the algorithm for each run. Figure 1b shows representative real-time ECG data collected during a *Constant DI* run. Two checks were performed to demonstrate the successful implementation of *Constant DI* pacing. First, the difference between expected and actual *DI*, i.e., algorithm error, was calculated and was less than 8 ms across all experimental runs. Figure 1c displays the algorithm error quantified for all beats at each *DI*, for one representative *Constant DI* run. Second, for each *DI*, the ECG data acquired was also analyzed post experiment and the T-wave peak detected by the algorithm was compared to the visible T-wave peak on the ECG to ensure accurate detection (Fig. 1b). Any run that incorrectly detected a T-wave or missed the expected *DI* by more than 8 ms due to technical limitations of the current study was excluded from further analysis. Details of the runs excluded are provided in the Supplementary Materials.

Presence and Onset of Alternans

We quantified the number of pacing runs that exhibited alternans in the heart for each pacing protocol and the corresponding BCL_{onset}, for both LV and RV. As seen in Fig. 2a, *Constant DI* pacing significantly reduced the instances of cardiac alternans in the heart (only 1 run demonstrated the presence of alternans for $DI = 40$ ms in the RV), compared to the other three pacing protocols. *Periodic* and *HRV* pacing always induced alternans and also had instances of VF. Furthermore, comparing BCL_{onset} between the *Periodic* and *HRV* pacing techniques (Fig. 2b), we observed that the onset of alternans in both the LV and RV is promoted with an increase in stochasticity in pacing, and *Physiological* pacing showed the largest BCL_{onset}. In case of the RV, *Periodic* pacing had significantly smaller BCL_{onset} in comparison to both *Gaussian* and *Physiological* pacing.

Spatio-Temporal Evolution of Alternans

Next, we quantified the spatial evolution of alternans for the different pacing protocols as a percentage of RV or LV areas occupied by alternans, for decreasing values of *DI*. Since *Physiological* pacing significantly preponed BCL_{onset} compared to both *Gaussian* and *Periodic* pacing, we only show data comparing *Periodic*, *Gaussian* and *Constant DI* from here on. Figure 3 shows representative 2D APD_{EVEN} and APD_{ODD} maps along with 2D alternans maps for decreasing *BCL*s and *DI*s, for *Periodic*, *Gaussian* and *Constant DI* pacing. For both *Periodic* and *Gaussian* pacing, we observed an increase in the area of the heart occupied by alternans as we decreased the *BCL* (shown in terms of calculated corresponding *DI*s), as demonstrated in Fig. 4. Note that *Constant DI* pacing prevented the spatio-temporal evolution of alternans in both LV and RV.

APD Heterogeneity μ

Figure 5 demonstrates the change in APD heterogeneity μ with a decrease in DIs for the three pacing protocols, along with representative 2D APD maps. There were no significant differences in μ between the three pacing protocols, although we observed a slightly higher μ in the RV during *Gaussian* pacing, in comparison to *Periodic* and *Constant DI* pacing. Representative 2D APD maps for all three pacing protocols are shown in Fig. 5 for a DI of ~ 50 ms.

APD Restitution Curve

Figure 6 shows APD_{80} as a function of different *DI*s for *Periodic*, *Gaussian* and *Constant DI* protocols.

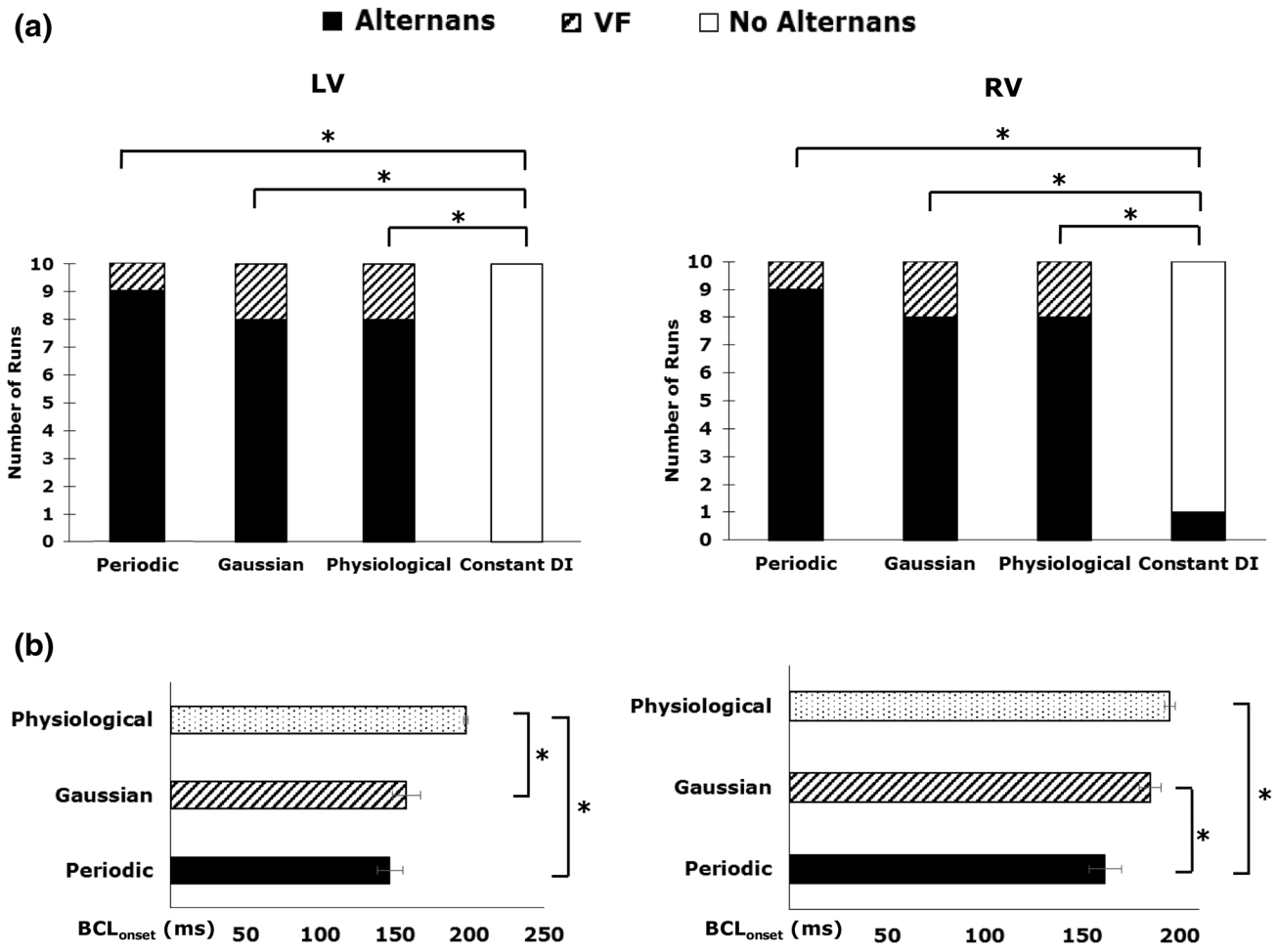

FIGURE 2. (a) Quantification of the occurrence of alternans in the heart for different pacing protocols. (b) Comparison of BCL_{onset} between *Periodic*, *Gaussian* and *Physiological* pacing. Asterisk denotes statistical significance of $p < 0.05$.

Constant DI pacing significantly lowered S_{max} in both the LV and RV in comparison to other pacing protocols. It is important to note that both *Periodic* and *Gaussian* pacing had $S_{max} > 1$ for both LV and RV, while $S_{max} < 1$ during *Constant DI* pacing, demonstrating its anti-arrhythmic effect. In addition, the calculated DI_{min} for the *Gaussian* pacing was significantly larger compared to *Constant DI* pacing for the LV (Fig. 6 bottom panel).

DISCUSSION

Here, we extended our previous *in silico* findings of the anti-arrhythmic benefits of *Constant DI* pacing[18,31] to the whole heart level and implemented a novel real-time closed loop system for beat-by-beat cardiac control. Using our system, we investigated the effect of feedback on the propensity to cardiac alternans, using three different pacing protocols: *Periodic* (feedback inherent), *HRV* (feedback modulation) and *Constant DI* (feedback elimination). Our major findings are as follows: First, we successfully implemented an algorithm for real-time detection of T-waves and validated its efficacy in controlling the *DI* on a beat-to-beat basis in the heart. Second, *Constant DI* pacing prevented the occurrence of alternans in the heart, thus providing a clear anti-arrhythmic effect. *Constant DI* pacing was associated with an increase in *APD* and decrease in S_{max}, while not affecting spatial heterogeneity of *APD*, μ, in comparison to *Periodic* pacing. On the other hand, feedback modulation using *HRV* pacing, which was modeled with either *Gaussian* or *in vivo Physiological* patterns, promoted the formation of alternans and VF in the heart, thus enhancing arrhythmogenicity. *HRV* pacing was associated with both increased S_{max} and μ, and earlier occurrence of alternans (larger BCL_{onset}), in comparison to *Periodic* pacing, thus providing clear pro-arrhythmic effects.

Our results support our hypothesis that the presence of feedback, or dependence of the *DI* on the preceding *APD*, can lead to electrical instability and cardiac

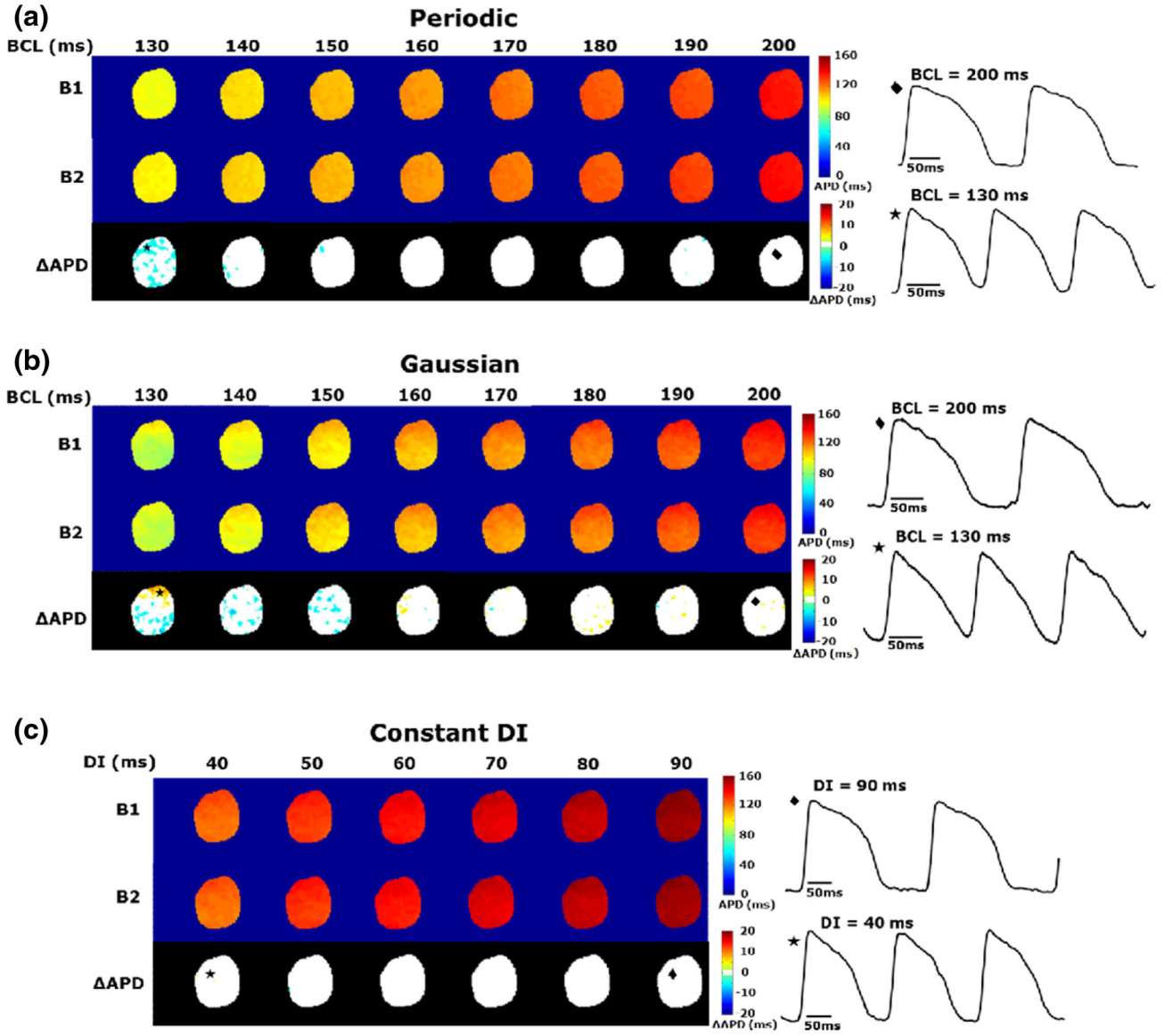

FIGURE 3. Representative 2D *APD* maps for APD_{EVEN} (B1), APD_{ODD} (B2) and ΔAPD (alternans), for (a) *Periodic*, (b) *Gaussian* and (c) *Constant DI* pacing, from the LV. Action potential traces depicting alternans (asterisk) at lower *BCL* and no alternans (filled diamond) at higher *BCL* are shown for *Periodic* and *Gaussian* pacing. Note that no alternans were observed for *Constant DI* pacing and representative action potential traces at two distinct *DI*s are denoted by asterisk and filled diamond.

arrhythmias, especially at higher pacing rates. This was demonstrated by the onset of spatio-temporal cardiac alternans during all *Periodic* pacing runs. Feedback modulation or *HRV* further perturbed the stability of the system and promoted arrhythmogenesis. To incorporate *HRV* in pacing, we used two methods. *Gaussian* distribution with 5% *HRV* was used to introduce perturbations in *BCL*, based on previously shown human *HRV* values and distributions.[18,23] Furthermore, to investigate a truly 'random' yet physiological perturbation, we also implemented *Physiological* pacing by utilizing RR interval patterns from previously recorded *in vivo* rat ECG traces. However, our results demonstrated an increase in arrhythmogenicity during *HRV* pacing, with *Physiological* pacing showing earlier onset of alternans than *Gaussian* pacing. This can be attributed to the fact that incorporating *HRV* in pacing only modulates feedback and does not eliminate the dependence of the *DI* on prior perturbations. *Constant DI* pacing however, ensures that the *DI* during each beat is independent of any prior instabilities or perturbations in the *APD* and hence, is more electrically stable.

HRV pacing also showed an increase in *APD* heterogeneity compared to both *Periodic* and *Constant DI* pacing. Since the beat-to-beat intervals are varied

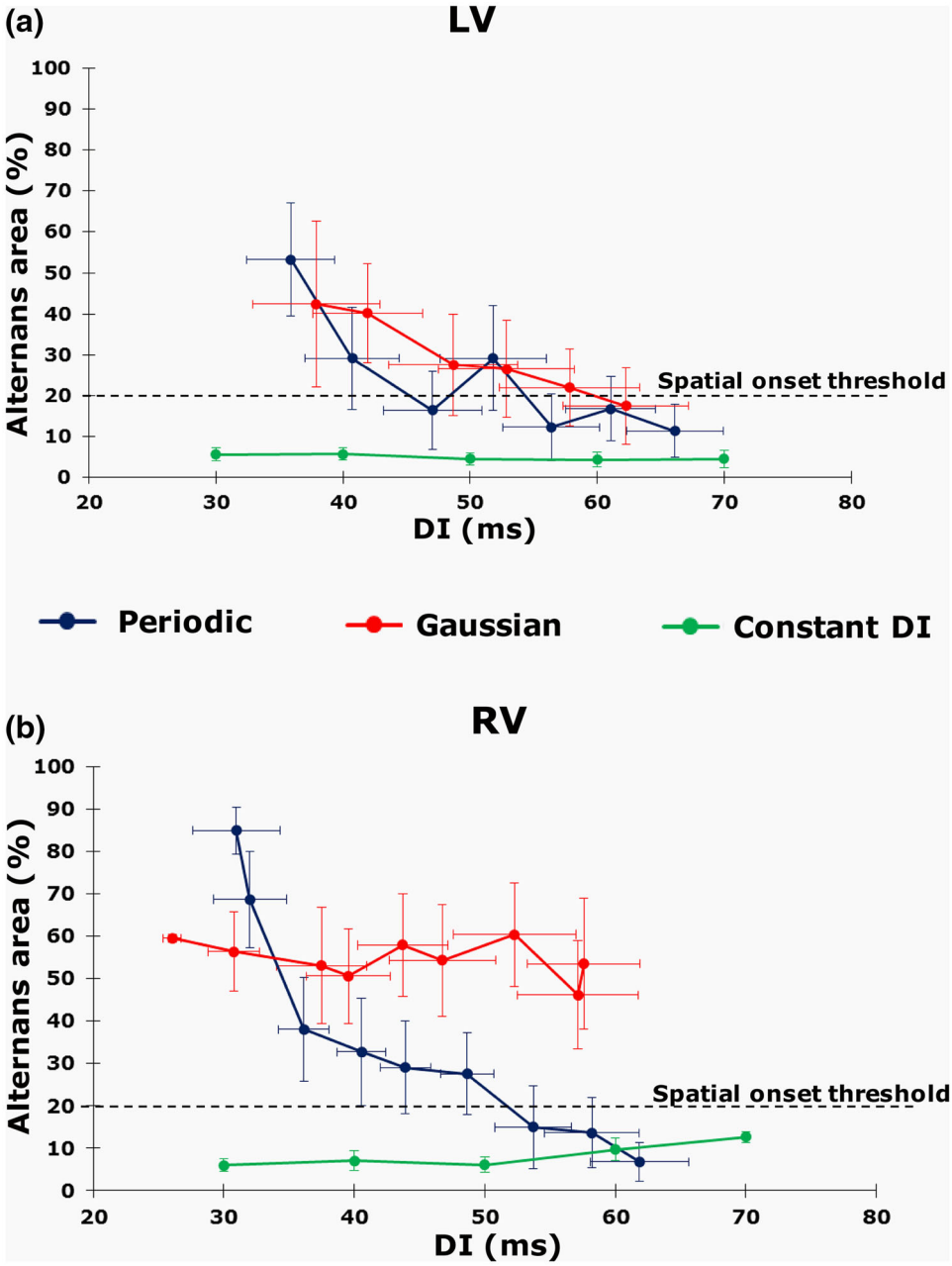

FIGURE 4. Spatial evolution of alternans across the (a) LV and (b) RV surfaces of the heart as *DI* decreases, for *Periodic* (blue), *Gaussian* (red) and *Constant DI* (green) pacing protocols. Dotted black line indicates the threshold used for spatial onset of alternans, i.e., BCL_{onset}.

randomly when incorporating *HRV* in pacing, it is possible that *APD* repolarization is heterogeneously affected. While certain regions might fully repolarize, other regions might be forced to reactivate before complete repolarization, which eventually could lead to heterogeneity in *APD* distribution across the surface of the heart. This could lead to abnormal activations such as early after depolarizations and delayed after depolarizations, which are known to be arrhythmogenic. This is supported by our data wherein we observed earlier onset of alternans, instances of VF and an earlier loss of pacing response (conduction block) during *HRV* pacing, demonstrated by a significantly larger DI_{min} in case of the LV.

Constant DI pacing also demonstrated a flattening in the slope of restitution. Numerous studies have suggested the anti-arrhythmic effects of flattening the restitution slope.[1,12,25] Expectedly, our data showed significantly steeper restitution curves during *Periodic* and *HRV* pacing, wherein we see an onset of alternans.

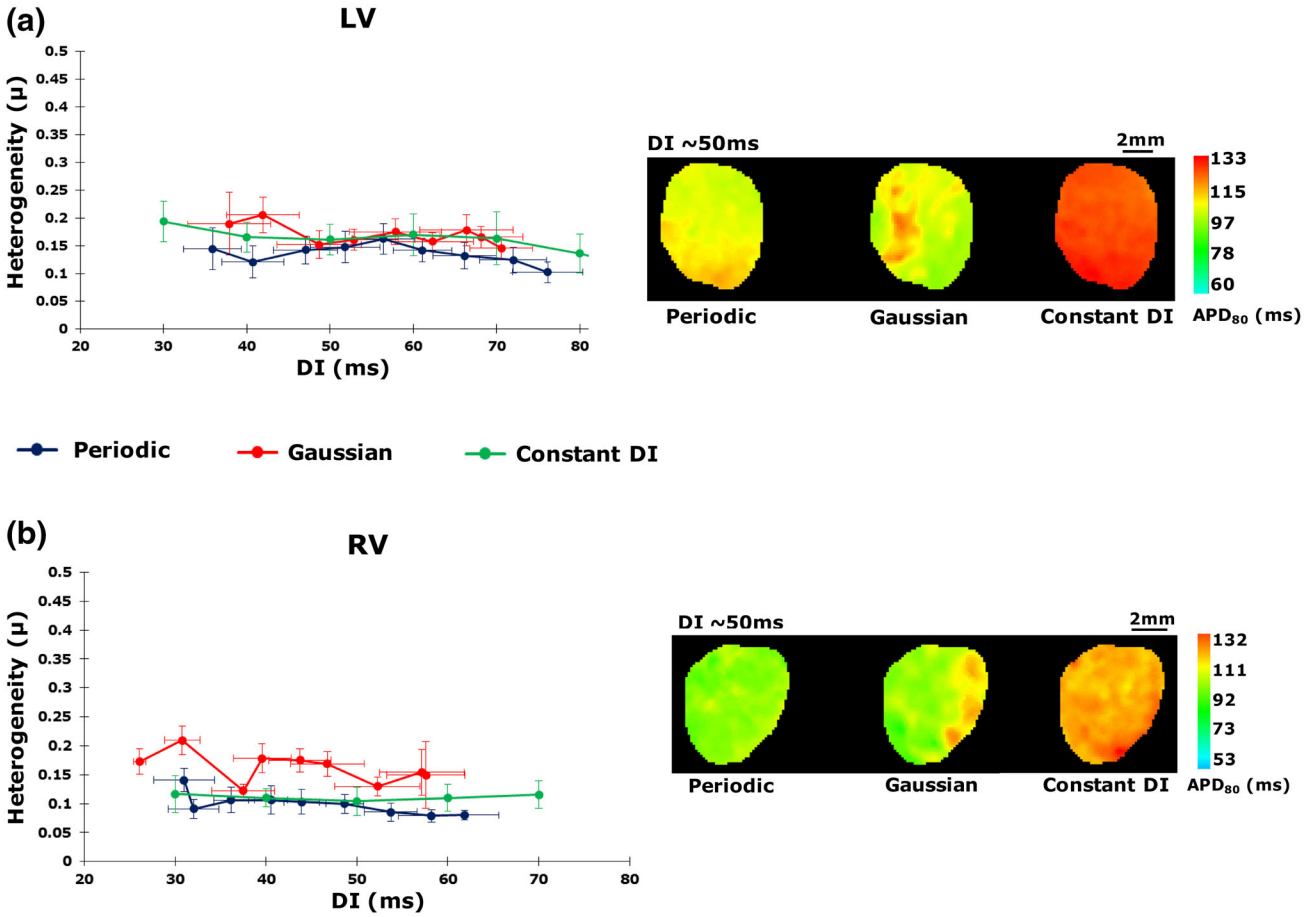

FIGURE 5. Change in APD_{80} heterogeneity μ with decreasing *DI*s for *Periodic* (blue), *Gaussian* (red) and *Constant DI* (green) pacing, for both (a) LV and (b) RV. Representative 2D *APD* maps are shown alongside for each pacing protocol, demonstrating the distribution of APD_{80} across the ventricles for a calculated *DI* of ~ 50 ms.

Since *Constant DI* pacing aims to maintain a fixed *DI* during each heartbeat, we saw an almost linear decrease in *APD* as we shortened our target *DI*, again demonstrating the beneficial effects of feedback elimination. Overall, our data shows promising anti-arrhythmic effects of feedback elimination and beat-to-beat *DI* control. Furthermore, all of our findings were consistent between the LV and RV and we did not observe any significant differences between ventricles in terms of the anti-arrhythmic benefits of *Constant DI* pacing.

LIMITATIONS

There are some limitations of the current study. First, we utilized volume conducted 3-electrode ECG that was easy to integrate with an existing 2D *ex vivo* optical mapping system, to implement *Constant DI* pacing. Hence, our study is limited by the temporal resolution achieved by volume conducted ECG and observing a distinct T-wave. Given the rabbit model and *ex vivo* setup, at very high pacing rates, the T-wave cannot be discerned, making it difficult to precisely detect the *DI*. However, feedback elimination can still be achieved by detecting a T-wave and incorporating a time offset in the target *DI*. Hence, the minimum *DI* successfully implemented was 30 ms for our study. Second, we used healthy rabbit hearts for our study and hence, the size of the hearts limits the spatial validation of the pacing techniques. Further pre-clinical validation would be required to explore the benefits of *Constant DI* pacing in a large animal model, as well as under diseased conditions. While similar ECG based approaches can be used for sensing T-waves and applying constant TR intervals in larger animals, the size of the heart could limit the spatial control achievable from single point pacing. Hence, there may be a need to utilize multi point intracardiac recordings for sensing instead of average ECG (which could mask local activity) for better spatio-temporal control in larger hearts. However, since rabbits are known to have electrical and ionic characteristics similar to humans, we do not expect a change in model to significantly alter the concepts established in this study.

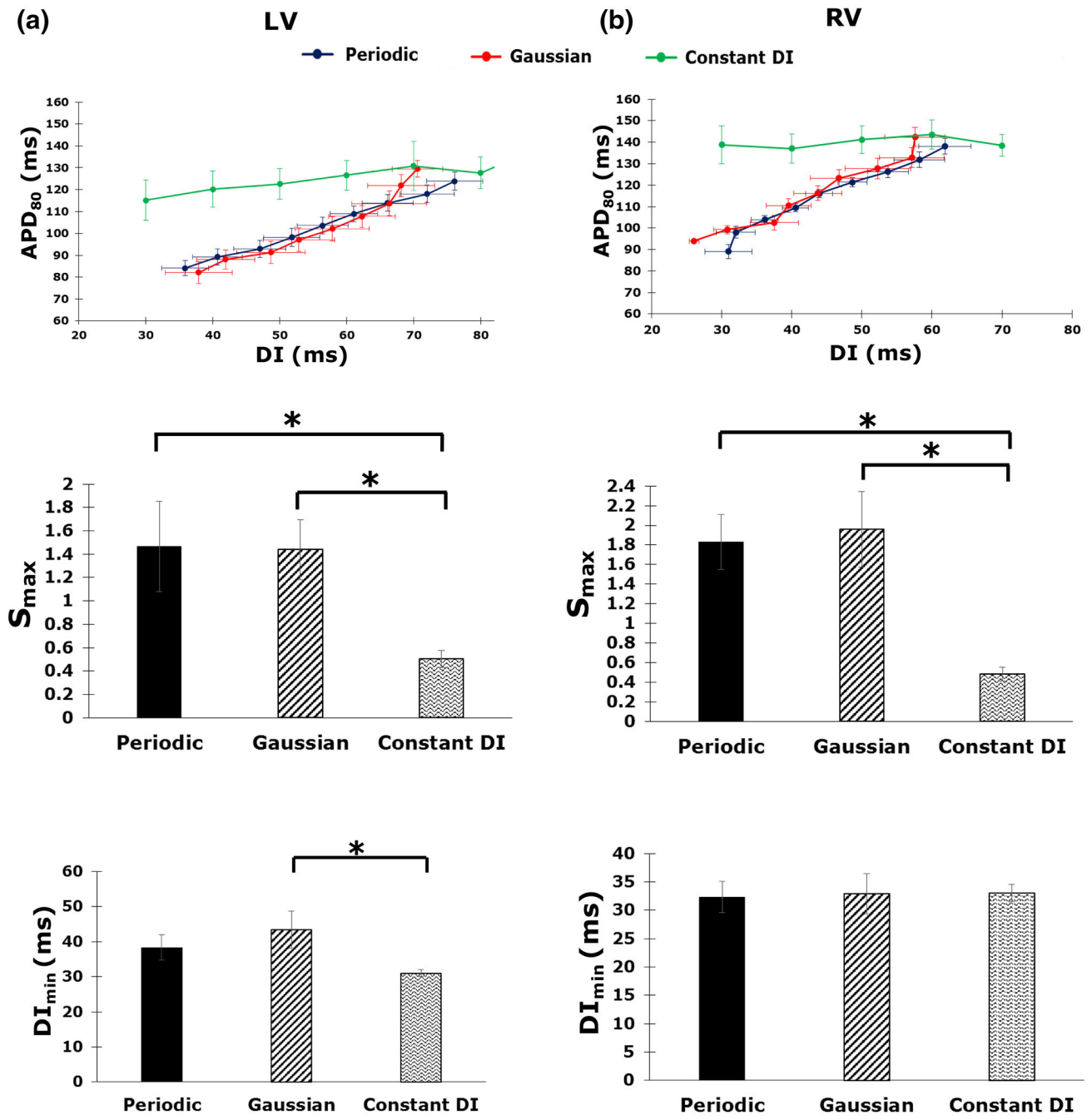

FIGURE 6. Top: Restitution curves demonstrating change in mean APD_{80} with decreasing *DI*s for *Periodic* (blue), *Gaussian* (red) and *Constant DI* (green) pacing. Mid: Maximum restitution slopes S_{max} calculated at DI_{min}. Bottom: Mean DI_{min} across all runs. Data shown for (a) LV (left panel) and (b) RV (right panel). Asterisk denotes statistical significance of $p < 0.05$.

In addition, to implement *Physiological* pacing, we utilized *in vivo* rat ECG rather than pre-recorded rabbit data. While species related differences in the RR interval patterns may be present, these differences may not be very relevant as the main focus of the current study was to investigate the effects of feedback modulation vs. feedback elimination. Our data demonstrates that variability, irrespective of the model used to implement it (Gaussian or Physiological) seems to be pro-arrhythmic. Finally, while our study demonstrates the efficacy of *Constant DI* in preventing restitution dependent alternans by eliminating feedback, it's effect on alternans driven by calcium cycling abnormalities remains unclear, and needs to be experimentally investigated in future studies.

CONCLUSIONS

We developed a novel real-time closed loop system to successfully validate the efficacy of *Constant DI* pacing in suppressing alternans using isolated whole hearts, hence demonstrating its potential in the prevention and control of cardiac arrhythmias. While the presence of feedback between the *DI* and *APD*, as demonstrated by use of *Periodic* pacing, induced cardiac alternans at higher pacing rates, incorporating *HRV* in pacing further enhanced the electrical instabilities and promoted the onset of alternans. In addition, irrespective of the model used to incorporate *HRV* in pacing, i.e., *Gaussian* or *Physiological* pattern, incorporating stochasticity in pacing showed pro-arrhythmic effects. Hence, our data suggests that feedback elimination using *Constant DI* might be essential in the prevention of restitution dependent cardiac alternans.

ELECTRONIC SUPPLEMENTARY MATERIAL

The online version of this article (https://doi.org/10.1007/s10439-018-1981-2) contains supplementary material, which is available to authorized users.

ACKNOWLEDGMENTS

This study was funded by the National Institute of Health F31HL129544 (to S.W.L.) and R21HL128790 (to E.G.T.), National Science Foundation CAREER PHY-125541 and DCSD 1662250. This work was conducted as a part of the Prediction and Control of Cardiac Alternans Working Group at the National Institute for Mathematical and Biological Synthesis, sponsored by the National Science Foundation through NSF Award #DBI-1300426.

CONFLICT OF INTEREST

The authors declare no conflict of interest.

REFERENCES

[1]Banville, I., and R. A. Gray. Effect of action potential duration and conduction velocity restitution and their spatial dispersion on alternans and the stability of arrhythmias. *J Cardiovasc. Electrophysiol.* 13(11):1141–1149, 2002.

[2]Cherry, E. M. Distinguishing mechanisms for alternans in cardiac cells using constant-diastolic-interval pacing. *Chaos* 27(9):093902, 2017.

[3]Christini, D. J., and J. J. Collins. Using chaos control and tracking to suppress a pathological nonchaotic rhythm in a cardiac model. *Phys. Rev. E.* 53(1):R49–R52, 1996.

[4]Christini, D. J., M. L. Riccio, C. A. Culianu, J. J. Fox, A. Karma, and R. F. Gilmour, Jr. Control of electrical alternans in canine cardiac purkinje fibers. *Phys. Rev. Lett.* 96(10):104101, 2006.

[5]Echebarria, B., and A. Karma. Spatiotemporal control of cardiac alternans. *Chaos* 12(3):923–930, 2002.

[6]Fox, J. J., J. L. McHarg, and R. F. Gilmour, Jr. Ionic mechanism of electrical alternans. *Am. J. Physiol. Heart Circ. Physiol.* 282(2):H516–H530, 2002.

[7]Garzón, A., R. O. Grigoriev, and F. H. Fenton. Model-based control of cardiac alternans on a ring. *Phys. Rev. E Stat. Nonlinear Soft Matter Phys.* 80(2):021932, 2009.

[8]Garzón, A., R. O. Grigoriev, and F. H. Fenton. Model-based control of cardiac alternans in Purkinje fibers. *Phys. Rev. E Stat. Nonlinear Soft Matter Phys.* 84(4):041927, 2011.

[9]Garzón, A., R. O. Grigoriev, and F. H. Fenton. Continuous-time control of alternans in long Purkinje fibers. *Chaos* 24(3):033124, 2014.

[10]Gilmour, Jr, R. F. Electrical restitution and ventricular fibrillation: negotiating a slippery slope. *J. Cardiovasc. Electrophysiol.* 13:1150–1151, 2002.

[11]Hall, K., D. J. Christini, M. Tremblay, J. J. Collins, L. Glass, and J. Billette. Dynamic control of cardiac alternans. *Phys. Rev. Lett.* 78:4518, 1997.

[12]Hall, G. M., and D. J. Gauthier. Experimental control of cardiac muscle alternans. *Phys. Rev. Lett.* 88(19):198102, 2002.

[13]Jordan, P. N., and D. J. Christini. Adaptive diastolic interval control of cardiac action potential duration alternans. *J. Cardiovasc. Electrophysiol.* 15(10):1177–1185, 2004.

[14]Kanu, U. B., S. Iravanian, R. F. Gilmour, and D. J. Christini. Control of action potential duration alternans in canine cardiac ventricular tissue. *IEEE Trans. Biomed. Eng.* 58(4):894–904, 2011.

[15]Karma, A. Electrical alternans and spiral wave breakup in cardiac tissue. *Chaos* 4(3):461–472, 1994.

[16]Kulkarni, K., R. Visweswaran, X. Zhao, and E. G. Tolkacheva. Characterizing spatial dynamics of bifurcation to alternans in isolated whole rabbit hearts based on alternate pacing. *Biomed. Res. Int.* 2015:170768, 2015.

[17]Malik, M. Heart rate variability. *Ann. Noninvasive Electrocardiol.* 1:151–181, 1996.

[18]McIntyre, S. D., V. Kakade, Y. Mori, and E. G. Tolkacheva. Heart rate variability and alternans formation in the heart: the role of feedback in cardiac dynamics. *J. Theor. Biol.* 350:90–97, 2014.

[19]Otani, N. F. Theory of the development of alternans in the heart during controlled diastolic interval pacing. *Chaos* 27(9):093935, 2017.

[20]Rappel, W. J., F. Fenton, and A. Karma. Spatiotemporal control of wave instabilities in cardiac tissue. *Phys. Rev. Lett.* 83:456, 1999.

[21]Riccio, M. L., M. L. Koller, and R. F. Gilmour. Electrical restitution and spatiotemporal organization during ventricular fibrillation. *Circ. Res.* 84(8):955–963, 1999.

[22]Sato, D., and C. E. Clancy. Cardiac electrophysiological dynamics from the cellular level to the organ level. *Biomed. Eng. Comput. Biol.* 5:69–75, 2013.

[23]Sookan, T., and A. J. McKune. Heart rate variability in physically active individuals: reliability and gender characteristics. *Cardiovasc. J. Afr.* 23(2):67–72, 2012.
[24]Stauss, H. M. Heart rate variability. *Am. J. Phys. Regul. Integr. Comp. Physiol.* 285(5):R927–R931, 2003.
[25]Tolkacheva, E. G., M. M. Romeo, M. Guerraty, and D. J. Gauthier. Condition for alternans and its control in a two-dimensional mapping model of paced cardiac dynamics. *Phys. Rev. E Stat. Nonlinear Soft Matter Phys.* 69(3 Pt 1):031904, 2004.
[26]Tolkacheva, E. G., and X. Zhao. Nonlinear dynamics of periodically paced cardiac tissue. *Nonlinear Dyn.* 68:347–376, 2012.
[27]Tse, G., S. T. Wong, V. Tse, Y. T. Lee, H. Y. Lin, and J. M. Yeo. Cardiac dynamics: alternans and arrhythmogenesis. *J. Arrhythm.* 32(5):411–417, 2016.
[28]Visweswaran, R., S. D. McIntyre, K. Ramkrishnan, X. Zhao, and E. G. Tolkacheva. Spatiotemporal evolution and prediction of $[Ca^{(2+)}]_i$ and APD alternans in isolated whole rabbit hearts. *J. Cardiovasc. Electrophysiol.* 24(11):1287–1295, 2013.
[29]Watanabe, M., N. F. Otani, and R. F. Gilmour, Jr. Biphasic restitution of action potential duration and complex dynamics in ventricular myocardium. *Circ. Res.* 76(5):915–921, 1995.
[30]Wu, R., and A. Patwardhan. Mechanism of repolarization alternans has restitution of action potential duration dependent and independent components. *J. Cardiovasc. Electrophysiol.* 17(1):87–93, 2006.
[31]Zlochiver, S., C. Johnson, and E. G. Tolkacheva. Constant DI pacing suppresses cardiac alternans formation in numerical cable models. *Chaos* 27(9):093903, 2017.